Organic & Biomolecular Chemistry

COMMUNICATION

View Article Online
View Journal | View Issue

CrossMark click for updates

Cite this: *Org. Biomol. Chem.*, 2015, **13**, 3856

Received 24th December 2014,
Accepted 17th February 2015

DOI: 10.1039/c4ob02659d

www.rsc.org/obc

Stapling monomeric GCN4 peptides allows for DNA binding and enhanced cellular uptake†

Abhishek Iyer,[a] Dorien Van Lysebetten,[a] Yara Ruiz García,[a] Benoit Louage,[b] Bruno G. De Geest[b] and Annemieke Madder*[a]

The basic DNA recognition region of the GCN4 protein comprising 23 amino acids has been modified to contain two optimally positioned cysteines which have been linked and stapled using cross-linkers of suitable lengths. This results in stapled peptides with a stabilized α-helical conformation which allows for DNA binding and concurrent enhancement of cellular uptake.

Introduction

Transcription factors (TFs) by definition are responsible for the decoding of genetic information from dsDNA to mRNA.[1] In the quest for DNA recognition, TF proteins can be taken as models to design synthetic DNA binders. They are usually classified according to the fold of their DNA-binding domains and grouped into a small number of families, like the bZIP, bHLH, homeodomain, HTH, and zinc fingers which have already been studied in detail.[2] Most transcription factors are large proteins possessing complex secondary structures rendering it difficult to design smaller synthetically accessible versions thereof retaining the DNA binding capacity.[3] The GCN4 leucine zipper is however a relatively easy protein to mimic due to its well-defined dimerization domain and basic recognition region.

It has already been shown that dimerization of basic region peptides through non-peptide scaffolds can allow DNA binding.[4] However, construction of such smaller dimeric mimics of this TF, although feasible, has proven to be synthetically challenging.[5,6] Previous attempts at more thorough structural minimisation and reduction of complexity using the monomeric GCN4 peptide have shown that DNA binding is greatly reduced due to loss of secondary structure.[7] Indeed, since the basic region of the GCN4 transcription factor cannot adopt a helical fold in solution by itself nor bind to DNA[8] due to entropic reasons,[9] an external factor forcing the peptide into a helical conformation is needed. For this reason unlike the existing synthetic bZip models in which DNA binding is induced *via* dimerisation,[5,10] we here aim to stabilize a single α helix *via* peptide stapling, reasoning that enhancing the helicity within the monomer should sufficiently stabilize the conformation to allow DNA binding.[7] Stapled peptides have been used extensively for improving helicity,[11] increasing cell-penetration,[12,13] proteolytic stability and enhancing peptide–protein interactions (PPIs).[14] In all the above mentioned cases the benefits of stapled peptides have been demonstrated.[15] However, the use of stapled peptides in the miniaturisation of zipper proteins has remained largely unexplored.

Results and discussion

In this work, we have examined the DNA binding induced by stapling using the monomeric GCN4 transcription factor basic region as a model peptide, by comparing the i, $i+4$ and i, $i+7$ stapling methods and varying the positions of the staple along the helix. The cellular uptake of the constructs was also investigated using fluorescently labelled versions of the peptide.

Selection of the stapling methodology

Initial studies were dedicated to selecting the most suitable method for peptide stapling among the ones reported in literature.[12,16–19] The idea was to adopt a method as general as possible to be applicable to any potential DNA binding peptide by increasing its helicity. To ensure easy and cost-effective modification the use of unnatural amino acids was avoided. Next to the labour-intensive preparation of the required modified amino acid building blocks, in case of the very well-known hydrocarbon stapling *e.g.*, coupling of the non-natural amino acids as well as peptide folding on resin has shown to give problems.[20] Therefore, in the current study we opted for cysteine cross-linking,[15] in view of the commercial availability and/or easy synthesis of cross-linking moieties,

[a]*Organic and Biomimetic Chemistry Research Group, Krijgslaan 281, S4, B-9000 Gent, Belgium. E-mail: annemieke.madder@ugent.be; Fax: +32-9-264 49 98*
[b]*Department of Pharmaceutics. Ghent University, Ottergemsesteenweg 460, 9000 Ghent, Belgium. E-mail: br.degeest@ugent.bel; Tel: +329 264 80 55*
†Electronic supplementary information (ESI) available: Experimental procedures, HPLC and NMR data. See DOI: 10.1039/c4ob02659d

mild reactions conditions and easy scalability due to synthesis in solution.

Design and synthesis of stapled peptides

A detailed analysis of the essential contacts for binding of the GNC4 protein to its cognate DNA sequence as derived from the reported crystal structure was described earlier by Ellenberger (pdb file: 1YSA).[21] Various dimeric peptides based on the D226-Q248 basic region of the GCN4 TF have been shown to retain their DNA binding properties.[10,22] Based on these studies, amino acids within this sequence, indicated as not involved in DNA contacts,[23] were identified and systematically replaced by Cys according to an *i*, *i* + 4 or *i*, *i* + 7 format. Molecular modelling aided visualisation based on the pdb file 1YSA[21] was used to ensure that the introduced linkers point away from the DNA and not towards it thereby avoiding any steric repulsion which may arise due to peptide stapling. In this way three different peptides, comprising the D226–Q248 sequence from the DNA binding basic region of GCN4, containing a double Cys substitution (at positions 237/244 for **1**, 229/233 for **2** and 233/237 for **3**) were synthesized on solid support, cleaved and subsequently treated with various linkers 1YSA yielding a series of five stapled peptides as shown in Fig. 1.

The stapled peptides and the unmodified WT basic region peptide were successfully synthesized. The cross-linkers **a**, **c** & **d** are commercially available. The stapling moiety **b** has not been used thus far for peptide stapling and was designed and synthesized as a more polar alternative to the biphenyl and bipyridine cross-linkers.

DNA binding studies

Next, the DNA binding capacity of all peptides was evaluated through electrophoretic mobility shift assay (EMSA) titration of various peptide concentrations to the DNA sequence 5′ – CGG ATG ACG TCA TTT TTT TTC – 3′ (Fig. 2) containing the cognate monomeric GCN4 binding site GTCAT. The WT peptide **4** does not bind DNA under the given EMSA conditions. For all the synthetic constructs **1a–c**, **2d** & **3d** we see enhanced DNA binding as compared to peptide **4**. Earlier, DNA binding with monomeric peptides was observed through the use of a grafting strategy whereby the crucial contact residues of the GCN4 binding region are specifically positioned on an avian pancreatic polypeptide.[24] Apparently, our simple and straightforward stapling strategy also allows constraining the peptide into a suitable conformation for DNA binding. In the case of peptides **1a–c** binding is only observed at higher concentrations of peptide as compared to **2d** and **3d**. The more hydrophobic nature of the biphenyl cross-linker, makes peptide **1a** more susceptible to aggregation (followed by precipitation) as can be seen from the complete disappearance of the bands in the

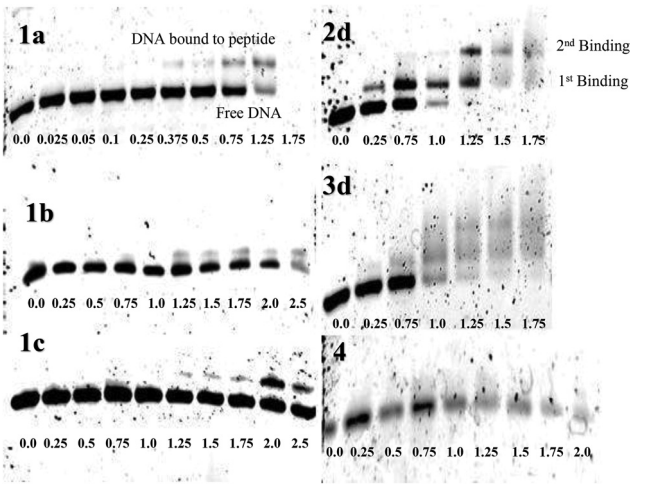

Fig. 2 EMSA titrations for peptides **1a–c**, **2d** & **3d**. Loading mixture comprises 5 μL from a mixture of 10 μL mQ, 4 μL sucrose, 2 μL loading buffer, 2 μL DNA, 2 μL peptide resulting in a total DNA concentration of 167 nM. The loading buffer consists of 20 μL Tris 1 M, pH = 7.6, 20 μL KCl 0.2 M, 20 μL $MgCl_2$ 0.1 M, 40 μL EDTA 0.025 M. Peptide concentrations from left to right (in μM) are indicated below each gel.

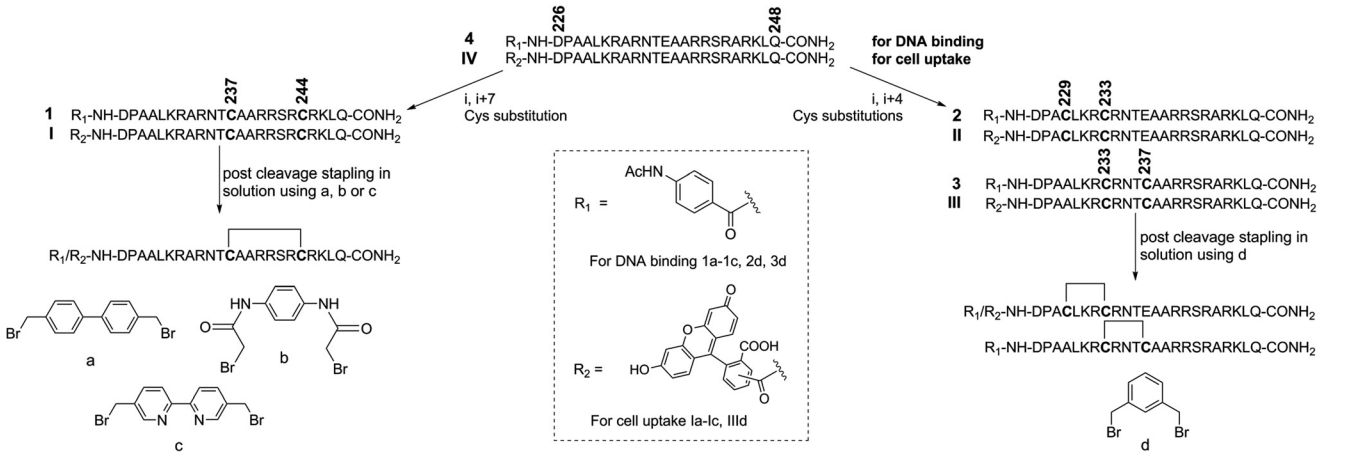

Fig. 1 Synthetic stapled peptides **1a–c**, **2d**, **3d** for DNA binding and unmodified basic region peptide **IV**. The peptides are N-terminally capped with a *p*-acetylamino benzoic acid (ABA) moiety to ensure UV-based detection and analysis in the case of DNA binding. For cell uptake studies the ABA moiety was replaced by fluorescein.

last lane. On the other hand, peptides **1b** and **1c** are less prone to aggregation but the onset of binding occurs at higher concentrations than in the case of **1a**. Compared to peptides **1a–c**, the DNA binding pattern in gel **2d** is different. We propose that the appearance of two bands related to DNA–peptide complex formation is due to the presence of two binding sites in the CRE sequence (...GTCAT...).

It can be noticed that after full occupation of one binding site by the peptide, remaining non-bound peptide can interact with the second binding site. The binding pattern of peptide **2d** is unique and only visible in the case of the two sequences that bind at a lower concentration range. It can further be noticed that peptide **3d** shows a similar binding pattern as peptide **2d** but suffers from non-specific interactions, which cause aggregation, bands getting blurred or disappearance of all bands.

From the few examples about DNA binding stapled described in literature[7,25] and from our own data we believe the major challenge in case of DNA binding peptides is that increasing the helicity has to be complemented with a degree of flexibility in order to account for the conformational change which occurs when the peptide binds to DNA. Since this conformational change is more significant in the case of DNA binding peptides as compared to PPIs, a too tight locking of the peptide into a helical conformation may result in the inability to achieve DNA binding. Indeed, our data show that peptide stapling by providing an N or C terminal helix stabilization, rather than centrally in the sequence, gives better results in terms of DNA binding as observed from the binding pattern of peptides **2d** & **3d** *versus* **1a–c**. Though in the absence of DNA, a low helical content is observed (see CD measurement results in ESI†) apparently the conformation can be adjusted into a structure whereby the contacts between the positively charged side chains, mainly involving the Lys and Arg residues, and the negatively charged backbone of the DNA can be maximized without a high entropic penalty. We believe peptide **2d** fits these criteria and hence is the best DNA binder from the constructs synthesized. Moreover, peptide **2d** is able to bind in a dimeric fashion without having been artificially dimerized.

Cell uptake & toxicity studies

The previously related yeast derived GCN4 peptide (231–252) has been classified as a membrane permeable peptide.[26,27] It varies slightly from the basic region peptide used in this article which was specifically chosen for its DNA binding abilities in its dimeric form.[22] It has further been postulated that stabilization of the secondary structure *via* peptide stapling can enhance cell uptake.[28] Peptides with hydrocarbon staples in particular have shown considerable increase in uptake as compared to their non-stapled counterparts.[13,29] Here, the fluorescently labelled versions of peptides **Ia–c** & **IId** were tested in a cellular environment using RAW 264.7 mouse macrophages. Confocal microscopy confirmed that cell uptake is achieved even at a low concentration of 0.25 μM for all peptides at 37 °C using an incubation time of 3 h, including

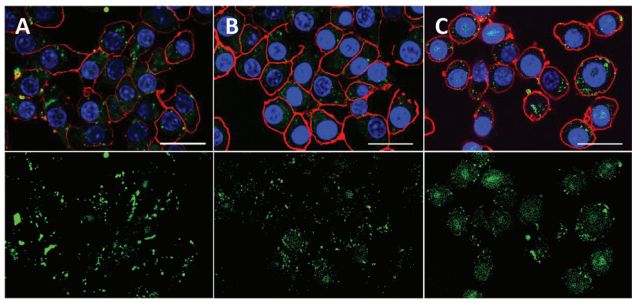

Fig. 3 Confocal microscopy images of the uptake of peptides (A) **Ib**, (C) **IId**, and (C) **IV** at 37 °C. The upper panel shows accumulated images of DNA in the nucleus (blue), cell membrane (red) and fluorescein (green). The lower panel shows the fluorescein image.

native GCN4 sequence **IV**, as can be seen from fluorescence of fluorescein in Fig. 3A–C.

Quantification of the uptake by flow cytometry shows a concentration dependence as well as a temperature dependence on the mean fluorescence values measured (Fig. 4). At 37 °C a considerably larger uptake is observed at a 1 μM concentration of peptides. Furthermore, the mean fluorescence of the cells increased considerably for an *i*, *i* + 7 staple as can be seen from the results for **Ia–c**. Incubation at 4 °C provides insight into the mode of uptake as endocytic pathways are shut down at this temperature. Comparison of the data obtained at 4 °C and 37 °C with flow cytometry (Fig. 4) showed that there is significant uptake at 37 °C but almost no uptake at 4 °C. This was further confirmed by confocal microscopy in a separate systematic study where we compared cell uptake for the non-stapled reference peptide **IV** and stapled peptide **Ib** both at 4 °C and 37 °C (Fig. 5). Except for slight accumulation in and around the cell membrane there was no uptake at 4 °C. Thus, active uptake is the main internalization pathway for these peptides based on the results obtained from flow cytometry and confocal microscopy.

The cell uptake properties even at low concentrations for the current peptides are combined with low cytotoxicity values

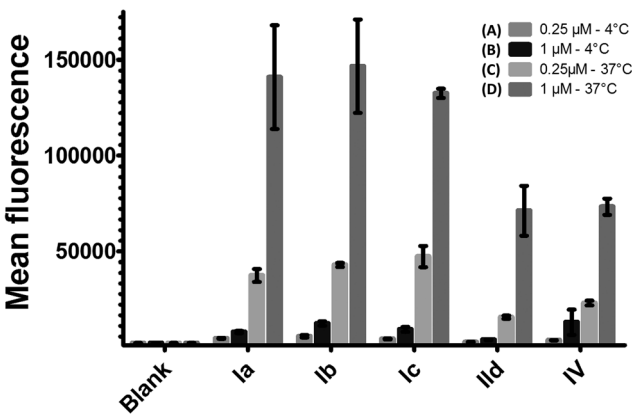

Fig. 4 Mean fluorescence of fluorescently labelled peptides by incubation at (A) 0.25 μM, 4 °C, (B) 1 μM, 4 °C, (C) 0.25 μM, 37 °C, (D) 1 μM, 37 °C.

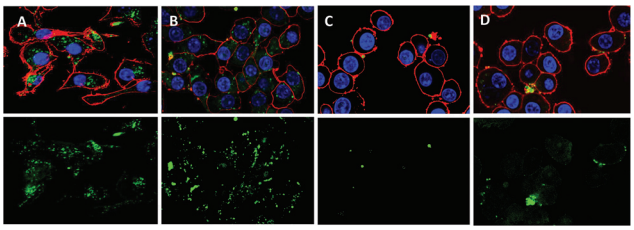

Fig. 5 Confocal microscopy images of the uptake of (A) peptide **IV** at 37 °C, (B) peptide **Ib** at 37 °C, (C) peptide **IV** at 4 °C and (D) peptide **Ib** at 4 °C at 0.25 μM. The upper panel shows accumulated images of DNA (blue), cell membrane (red) and fluorescein (green). The lower panel shows the fluorescein image.

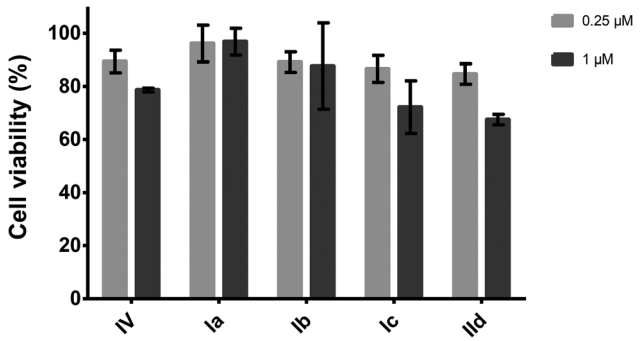

Fig. 6 MTT assay for fluorescently labelled peptides **IV**, **Ia**, **Ib**, **Ic** & **IId** measured at concentrations of 0.25 μM and 1 μM.

as observed in an MTT-assay (Fig. 6). From the MTT assay we can conclude that for peptides **IV**, **Ia**, **Ib**, **Ic** and **IId** in general more than 70% of the cells are viable at a concentration of 0.25 μM. Cell viability was evaluated according to the ISO10993-5 norms which state that the compounds are cytotoxic if the assay points to a cell viability lower than 70%. Clearly, we see that the stapled peptides are not toxic at a concentration of 0.25 or 1 μM except for **IId** which seems to be slightly toxic at a 1 μM concentration.

Peptide stability

Many hydrocarbon stapled peptides exhibit increased proteolytic resistance, proportional to the degree of α-helicity and number of staples introduced, resulting in enhanced therapeutic properties.[30] In case of cysteine cross-linking, no systematic comparison of peptide stability of stapled *versus* unstapled peptides has been reported. As a high number of Arg and Lys are present, the peptides will be very susceptible to cleavage of trypsin. Therefore a trypsin digest experiment was carried out using a trypsin to peptide ratio of 1/1000 wt% and samples were analysed after 0 min, 30 min, 1 h, 2 h and 24 h using RP-HPLC and MALDI-TOF. As expected, the control peptide **IV** was more susceptible to degradation than the stapled peptides which can be seen in the higher number of different degradation products (Fig. 7). The degradation products clearly reflect the influence of the staple on the cleavage process. Remarkably, while peptide **IV** was completely

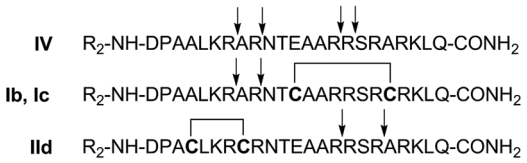

Fig. 7 Trypsin digest of peptides showing different cleavage sites indicated by the arrows, observed with RP-HPLC analysis.

degraded after 24 h, between 20% (**Ic**) and 80% (**Ib**) was left for the different stapled peptides (see Fig. 50 in ESI†).

Conclusions

The elegant nature of the synthesis in combination with the observed DNA binding and cellular uptake properties render these constructs of considerable and specific interest among the mimics of the GCN4 transcription factor reported to date. Through this work and due to the nature of the stapled peptides, we believe that a general method is now at our disposal to allow DNA binding and enhance cellular uptake of a given DNA binding peptide while avoiding tedious synthetic routes. It has been further shown that N-terminal helix stabilization as in the case of 2d is more effective for enhancing DNA binding than stapling in the middle of the sequence (**1a–c**). For cell uptake, however, the more helical *i*, *i* + 7 stapled peptides **Ia–c** have shown better uptake than **IV**. Although the two are not mutually exclusive, for future applications such as DNA binding *in cellulo*, a balance will have to be found between a peptide's DNA binding and cell penetration abilities.

Experimental

Materials

All amino acids, trifluoroacetic acid (TFA) and coupling reagent HBTU were purchased from Iris GmbH. L-Amino acids were used throughout the syntheses. The protecting groups for the amino acids are ^{t}Bu for Asp, Glu, Ser, Thr, Boc for Lys, Pbf for Arg and Trt for Cys, Asn, Gln. 4-Acetamidobenzoic acid (ABA), 4-4′-bis(bromomethyl)biphenyl, α,α′-dibromo-*m*-xylene, *p*-phenylenediamine, ethyl acetate, acetonitrile, methanol, diethyl ether, DIPEA, supplied as extra dry, redistilled, 99.5% pure and triisopropylsilane were purchased from Sigma Aldrich. Bromoacetylbromide was purchased from Acros Organics. Dimethylformamide (DMF) and *N*-methylpyrrolidine (NMP) peptide synthesis grade were purchased from Biosolve. HPLC grade quality hexane and chloroform were purchased from Fisher Scientific. Deuterated solvents D_2O (99.9% atom D) and DMSO-d6 (99.8% atom D) were obtained from Eurisotop. Water with the Milli-Q grade standard was obtained in-house either from a Millipore ROs 5 purification system or a Sartorius Arium 611 DI. Rink-Amide ChemMatrix (100–200 μm, manufacturer's loading: 0.52–0.54 mmol g^{-1}) was obtained from Biotage. NHS-fluorescein was purchased

from Thermo Scientific as a 5–6 isomer. All reagents were acquired from commercial sources and used without prior purification. All chemicals were used without further purification. All oligonucleotides used were commercially purchased from Eurogentec (HPLC purified using RP-cartridge-Gold, 200 nm scale) and were used as such.

Peptide syntheses

All automated peptide synthesis were performed using Rink Amide Chemmatrix resin, loading = 0.54 mmol g^{-1} on a 100 mg scale using 10 eq. of amino acid, 10 eq. of HBTU and 20 eq. of DIPEA in DMF using single couplings of 1 h. Fmoc deprotection was performed using 20% piperidine in DMF and shaking for 2, 5 and 15 min. For coupling fluorescein to the N-terminus 3 eq. of NHS fluorescein along with 3 eq. HOBt and 6 eq. of DIPEA was used and the reaction mixture was shaken overnight. The peptides were cleaved off using TFA–TIS–H_2O = 95/2.5/2.5 and precipitated using cold MTBE.

For peptide stapling, 10 mg of crude peptide was dissolved in 2–3 mL of NH_4HCO_3 solution (depending on the solubility) with 1.5 eq. of tris(2-carboxyethyl) phosphine (TCEP) and was stirred for 15 min at room temperature. Then 2.5 eq. of cross-linker dissolved in 1 mL of dry DMF was added drop-wise to the reaction mixture and was stirred for another 2–2.5 h after which the crude reaction mixture was analyzed by MALDI-TOF to observe the progress. If starting material was detected, 1.5 eq. of cross-linker in 1 mL dry DMF was added and the reaction was continued for another 1.5–2 h. MALDI-TOF samples were taken every 45 min. The solvents were removed and the peptides were obtained by precipitation (twice) by centrifugation at 4000 rpm at 0 °C in cold MTBE (−20 °C). The pellet was then redissolved in mQ H_2O and purified using RP-HPLC to give pure stapled peptides.

Electrophoretic mobility shift assay

The following stock solutions were prepared (fresh each time, except for DNA and peptide):

DNA: 1.67 μM prepared from CRE (5′ – CGG ATG ACG TCA TTT TTT TTC – 3′) & CRE complement (5′ – GAA AAA AAA TGA CGT CAT CCG – 3′) and Random (5′ – GCG CGA GAA GGA AAG AAA GCC GG – 3′) & complement (5′ – CCG GCT TTC TTT CCT TCT CGC GC – 3′) DNA solutions (commercially purchased) by diluting with 20 μL 0.5 M Tris, pH = 8, 40 μL 2.5 M NaCl, 40 μL 0.025 M EDTA and then adding milliQ water such that the total volume is 1 mL. The DNA was annealed by heating in a Thermomixer from room temperature to 95 °C and maintaining the temperature at 95 °C in total time of 24 min. The machine was then turned off and the sample was allowed to cool down slowly.

Loading buffer: 20 μL Tris 1 M, pH = 7.6, 20 μL KCl 0.2 M, 20 μL $MgCl_2$ 0.1 M, 40 μL EDTA 0.025 M.

Sucrose: 30% sucrose in mQ (300 mg mL^{-1}).

Peptides: 10 μL stock solutions (10×) were prepared in MilliQ water (0, 1.67, 5.01, 6.68, 7.51, 8.35, 10.02, 11.69, 13.36, 16.7 μM).

Loading mixture: The loading mixture comprised of: 10 μL mQ, 4 μL sucrose, 2 μL loading buffer, 2 μL DNA, 2 μL peptide. The loading mixture was prepared only 1–2 h prior to running of gels and kept on ice as soon as ready.

Preparation of Gels (for 2 Gels). In a clean falcon tube the following were added (in given order): 15.595 mL mQ, 0.4 mL TBE, 4.005 mL of 40% acrylamide solution, 200 μL APS (10% w/w in mQ). The solution was mixed by sonication to remove any air bubbles and cooled to 0 °C (1 h under ice). 20 μL of TEMED was then added to the mixture and was again mixed properly before pouring it gently along parallel glass plates. The glass plates were tapped gently to ensure removal of all air bubbles and the markers were squeezed between the plates to ensure uniform width of each well. Sufficient time was given for polymerization (~1 h).

Gel electrophoresis. A pre-run of the gels was performed prior to loading them. Care was taken to see that the gels were properly immersed in 0.2× TBE buffer (non-denaturing gel, without urea) and the loading wells were free from any air bubbles. Instrument settings: 150 V, 100 mA, 19 W for 30 min at 4 °C. The wells were washed after the pre-run. 5 μL of the loading mixture was then loaded onto the wells. Instrument settings: 150 V, 100 mA, 19 W for 45 min at 4 °C.

Staining of gels. After the run, the gels were removed from the glass and were stained using 100 mL of 0.2× TBE buffer + 10 μL Sybr Gold (commercially purchased stock solution 10 000× in DMSO). The gels were then washed twice with mQ and gently placed under a UV lamp (dark room) to observe the gel pattern.

Confocal microscopy

RAW264.7 cells cultivated in DMEM (10^5 per well, 300 μL) were plated in confocal plates and incubated overnight at 37 °C and 5% CO_2. Peptides were added in an overall concentration of 0.25 μM and incubated for 2 h at the same conditions or on ice. Cells were washed and fixated with 2% of Paraformaldehyde for 30 min at 37 °C. Cells were stained by 30 min incubation with a 0.2% solution of CTB-AF647 and 0.2% of Hoechst in PBS with 1% BSA. This was done to visualize the cell nucleus (blue) and cell membrane (red) respectively. Cells were resuspended in PBS and measured with confocal microscope (Leica SP5 equipped with a 63× (1.4 NA) oil immersion objective) at 3 different wavelengths (405 nm, 488 nm and 643 nm). The peptides used were labeled with fluorescein which emits green light. To understand the uptake mechanism better, three samples are made in duplicates and incubated at 4 °C to inhibit active transport. Due to the difference in emission wavelength, the three dyes can be detected separately. Processing the data with Image J gave overlay images whereby the nucleus, cell membrane and fluorescein are shown in blue, red and green respectively.

Flow cytometry

RAW264.7 cells cultivated in DMEM (10^5 per well, 1 ml) were plated in a 24-well plates and incubated overnight at 37 °C and 5% CO_2. Peptides were added in an overall concentration of

0.25 μM and 1 μM and incubated for 2 h at the same conditions or on ice. Cells were washed with PBS and detached with Na_4EDTA. Cells were re-suspended in PBS and added to the BD Accuri flow cytometer. Experiments were carried out in duplicate.

MTT assay

RAW264.7 cells cultivated in DMEM (10^4 per well, 200 μL) were plated in a 96-well plates and incubated overnight at 37 °C and 5% CO_2. The peptides and control compounds were added in an overall concentration of 0.25 μM and 1 μM and incubated for 24 h under the same conditions. The MTT solution was then added to the aspirated wells and incubated for 3 h. After removal of the cell medium, purple formazan crystals were dissolved in DMSO. Then, UV-measurement at 570 nm was performed with a plate reader to check cell viability quantitatively. An observation with the naked eye already gave a good idea about the toxicity of the compounds due to the disappearance of color in the well. Comparison of the absorbance of the formazan solution of the sample to the absorbance of a positive control (incubation with DMSO) and a negative control (incubation with ultrapure water) gave quantitative results of cell viability as in the equation:

$$\text{Cell viability}\,(\%) = \frac{A - A_{\text{pos}}}{A_{\text{neg}} - A_{\text{pos}}} \times 100$$

Peptide stability

Peptides dissolved in a 50 mM NH_4HCO_3 buffer at a concentration of 0.5 mg mL^{-1} are incubated at 37 °C with a trypsin solution (trypsin/peptide: 1/1000 wt%) in AcOH 50 mM buffer. The pH was optimized to 7–9. Samples were taken after 0 min, 30 min, 1 h, 2 h and 24 h and injected on RP-HPLC (Jupiter C4 300A, 0–100% CH_3CN in 15 min). Peaks were collected and analysed using MALDI-TOF. Peaks were integrated. The peak area at 0 min was used as control.

Acknowledgements

Tim Courtin is acknowledged for the determination of the concentration of the final compounds by ERECTIC-NMR. Ellen Gyssels is thanked for her assistance in determining the concentration of the DNA strands and fluorescently labeled peptides using the Trinean DropSense 96. Jan Goeman is acknowledged for the LC-MS analysis. Abhishek Iyer and Yara Ruiz García are indebted to the Marie Curie Early Stage Research Training Fellowship of the European Community's Seventh Framework Programme under contract number PITN-GA-2010-238679. The FWO and BOF are also acknowledged for financial support.

Notes and references

1 D. S. Latchman, *Eukaryotic Transcription Factors*, Elsevier, London, 5th edn, 2011, ch. 1, p. 1.
2 E. Pazos, J. Mosquera, M. E. Vázquez and J. L. Mascareñas, *ChemBioChem*, 2011, **12**, 1958–1973.
3 N. M. Luscombe, S. E. Austin, H. M. Berman and J. M. Thornton, *Genome Biol.*, 2000, **1**, 1–10.
4 L. L. G. Carrette, T. Morii and A. Madder, *Eur. J. Org. Chem.*, 2014, **14**, 2883–2891.
5 T. Morii, M. Simomura and S. Morimoto, *J. Am. Chem. Soc.*, 1993, **32**, 1150–1151.
6 A. M. Vázquez, M. Eugenio and J. L. Mascareñas, *Angew. Chem., Int. Ed.*, 2000, **112**, 3234–3237.
7 M. I. N. Zhang, B. Wu, H. Zhao and J. W. Taylor, *J. Pept. Sci.*, 2002, **136**, 125–136.
8 C. Park, J. L. Campbell and W. A. Goddard, *J. Am. Chem. Soc.*, 1996, **118**, 4235–4239.
9 L. K. Henchey, A. L. Jochim and P. S. Arora, *Curr. Opin. Chem. Biol.*, 2008, **12**, 22–26.
10 J. Mosquera, A. Jiménez-Balsa, V. I. Dodero, M. E. Vázquez and J. L. Mascareñas, *Nat. Commun.*, 2013, **4**, 1874.
11 K. Estieu-gionnet and G. Guichard, *Drug Discovery*, 2011, **6**, 937–963.
12 M. M. Madden, A. Muppidi, Z. Li, X. Li, J. Chen and Q. Lin, *Bioorg. Med. Chem. Lett.*, 2011, **21**, 1472–1475.
13 H. Inhibitor, H. Zhang, Q. Zhao, S. Bhattacharya, A. A. Waheed, X. Tong, A. Hong, S. Heck, F. Curreli, M. Goger, D. Cowburn, E. O. Freed and A. K. Debnath, *J. Mol. Biol.*, 2008, **378**, 565–580.
14 C. J. Brown, S. T. Quah, J. Jong, A. M. Goh, P. C. Chiam, K. H. Khoo, M. L. Choong, M. a. Lee, L. Yurlova, K. Zolghadr, T. L. Joseph, C. S. Verma and D. P. Lane, *ACS Chem. Biol.*, 2013, **8**, 506–512.
15 H. Jo, N. Meinhardt, Y. Wu, S. Kulkarni, X. Hu, K. E. Low, P. L. Davies, W. F. DeGrado and D. C. Greenbaum, *J. Am. Chem. Soc.*, 2012, **134**, 17704–17713.
16 Y.-W. Kim, T. N. Grossmann and G. L. Verdine, *Nat. Protoc.*, 2011, **6**, 761–771.
17 Ø. Jacobsen, H. Maekawa, N. Ge, C. H. Görbitz and P. Rongved, *J. Org. Chem.*, 2011, **76**, 1228–1238.
18 W. S. Horne, *Chem. Commun.*, 2011, **47**, 1–4.
19 Y. Demizu, N. Yamagata, S. Nagoya, Y. Sato and M. Doi, *Tetrahedron*, 2011, **67**, 6155–6165.
20 L. D. Walensky and G. H. Bird, *J. Med. Chem.*, 2014, **57**, 6275–6288.
21 T. E. Ellenberger, C. J. Brandl, K. Struhl and S. C. Harrison, *Cell*, 1992, **71**, 1223–1237.
22 A. Jimønez-balsa, E. Pazos, B. Martínez-albardonedo, J. L. Mascareñas and M. E. Vázquez, *Angew. Chem., Int. Ed.*, 2012, **51**, 8825–8829.
23 W. Keller, P. Ko and T. J. Richmond, *J. Mol. Biol.*, 1995, **254**, 657–667.
24 N. J. Zondlo and A. Schepartz, *J. Am. Chem. Soc.*, 1999, **121**, 6938–6939.
25 L. Guerrero, O. S. Smart, G. A. Woolley and R. K. Allemann, *J. Am. Chem. Soc.*, 2005, **127**, 15624–15629.

26 S. Futaki, T. Suzuki, W. Ohashi, T. Yagami, S. Tanaka, K. Ueda and Y. Sugiura, *J. Biol. Chem.*, 2001, **276**, 5836–5840.
27 Ü. Langel, *Handbook of Cell-Penetrating Peptides*, CRC Press, 2nd edn, 2006, ch. 25, p. 440.
28 A. Muppidi, Z. Wang, X. Li, J. Chen and Q. Lin, *Chem. Commun.*, 2011, **47**, 9396–9398.
29 W. Nomura, H. Aikawa, N. Ohashi, E. Urano, M. Métifiot, M. Fujino, K. Maddali, T. Ozaki, A. Nozue, T. Narumi, C. Hashimoto, T. Tanaka, Y. Pommier, N. Yamamoto, J. a. Komano, T. Murakami and H. Tamamura, *ACS Chem. Biol.*, 2013, **8**, 2235–2244.
30 L. D. Walensky and G. H. Bird, *J. Med. Chem.*, 2013, **57**, 6275–6288.